Proceedings of ISERME 2025
19-20 September 2025
https://doi.org/10.31705/ISERME.2025.27

Wahawa Geothermal Field: Subsurface Structure and Direct Use Potential

Durairajapillai[1] JJA, [*]Samaranayake[1] SA, Herath[2] HMAMC, Wasundara[1] RAS, Wijewardane[1] HO, Dahanayake[1] U, Prasanna[3] HMI, Subasinghe[4] ND

[1]Department of Physical Sciences, Faculty of Applied Sciences, Rajarata University of Sri Lanka, Mihintale, Sri Lanka

[2]Department of Chemical Sciences, Faculty of Applied Sciences, Rajarata University of Sri Lanka, Mihintale, Sri Lanka

[3]Faculty of Geomatics and Surveying, Sabaragamuwa University of Sri Lanka

[4]National Institute of Fundamental Studies, Kandy

[*]Corresponding author – amali@as.rjt.ac.lk

Abstract

Sri Lanka, mainly depends on non-renewable energy sources. It is essential to meet the country's energy demand by developing and adopting renewable sources. This study was conducted to assess the geothermal potential of Wahawa geothermal field through integrated geophysical and geochemical methods. The water samples collected from 12 locations of the field were used for the geochemical characterization. The geochemical characterization to calculate the reservoir temperature included in-situ measurements such as pH, electrical conductivity, and wellhead temperatures along with major anion and cation analysis using Ion Chromatography and Microwave Plasma-Atomic Emission Spectroscopy respectively. The gravity, magnetic and resistivity data obtained from the geophysical measurements were used in determining the geometry and the location of the heat source. Gravity, resistivity and magnetic results collectively supports the presence of a geothermal reservoir associated with the dolerite dyke intrusions. A hypothetical model was developed for the geothermal field using the geochemical and geophysical data obtained. The geothermometric calculations estimate the maximum reservoir temperature to be 186 °C, corresponding to an energy input of 697.2 kJ/mol. The Monte Carlo volumetric assessment shows with a 90% probability that the reservoir could produce 2.6 MWe over a period of 30 years.

Keywords: Geothermometry, Low-enthalpy system, Monte Carlo volumetric assessment, Resistivity profiling

1 Introduction

According to the Sri Lanka Sustainable Energy Authority (SLSEA), the nation's total energy demand in 2023 was approximately 14,000 GWh[1], with a significant portion, around 50%, met through imported fossil fuels. This reliance on imports costs the country an estimated USD 4 billion annually, exposing the economy to global price volatility and supply disruptions. The involvement of these energy sources has also made a considerable contribution to environmental pollution in Sri Lanka. Hence, the need for environmental friendly, pollution-free, renewable energy is very important. Solar and wind energy contribute significantly to the energy mix, and hydropower accounts for 30% of electricity generation. However, geothermal energy which is a sustainable, reliable, and locally available resource remains largely untapped in Sri Lanka.

Sri Lanka is located in the Indian Ocean, approximately 880 km north of the equator,

between North latitudes 5°55' and 9°55' and longitudes 79°42' and 81°52'. The country's geology is characterized by 350 km long north-south striking contacts of the Igneous, Highland and Vijayan complexes[1]. The geology of the island is made up of three main crustal units as Wanni complex (WC), Highland complex (HC), and Vijayan complex (VC). Figure 1 shows a simplified geological map of Sri Lanka.

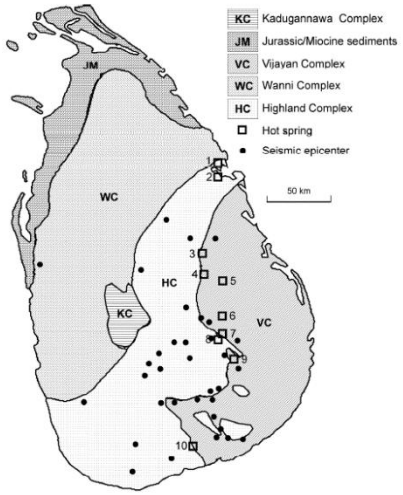

Figure ***1***: Geothermal hot springs in a generalized geological and tectonic map of Sri Lanka [1].

The most common hot springs are found in volcanic zones, where superheated water can reach the surface as steam or hot water. Some hot springs, however, are found in non-volcanic areas. This is because water percolates through the deep fracture zones and returning after being heated by a heat source or by a normal or above-normal geothermal temperature gradient. Even though Sri Lanka is not located near any active plate boundaries, or in an active volcanic region, Sri Lanka has ten geothermal spring fields in its Precambrian basement [2].

There are two major hypotheses explaining the origin of geothermal fields in Sri Lanka. One of them is that the Highland- Vijayan (H/V) boundary which is an inactive plate boundary passing through the country as a source of hot springs and the other hypothesis is that the dolerite dykes as a source of hot springs[3].

The study area Wahawa-Padiyatalawa is situated about 10 km South–East of Padiyatalwa town, southern part of the Ampara District, in the eastern province of Sri Lanka[4]. In the pastoral village of Wahawa in Padiyatalawa, eighteen hot water springs are scattered throughout the village[5]. Thermal spring temperatures range from 50 °C to 60 °C[6], and so far only limited preliminary scientific research has been carried out without detailed geological studies, geophysical surveys and test drilling. The origin of the geothermal source is yet to be explored[7][8].

The study focuses on assessing the geothermal potential of the Wahawa geothermal field through integrated geochemical and geophysical methods.

2 Methodology

2.1 Materials

The water samples were collected from 12 locations as shown in table 1 of the geothermal field in the Wahawa-Padiyatalawa area situated in Ampara district. These locations include samples from both thermal and non-thermal springs in the close proximity. Out of these, six samples were collected from hot water springs and the rest were collected from the cold springs and streams of the field. Two aliquots of samples were collected from each location with field blanks. One set of samples were collected to 200 mL bottles and were stored at 4 °C, in a refrigerator. The other set of samples were also collected to 200 mL bottles, acidified with 99% pure nitric acid to pH<2 to prevent precipitation and were stored at room temperature for further analysis.

Table 1: Background information on sampling sites

Locations	Geographic coordinates	
	North	East
Hot spring 1	239667	259119
Hot spring 2	296606	259222
Hot spring 3	239589	259294
Hot spring 4	239654	259312
Hot spring 5	239466	259445
Hot spring 6	239857	259219
Cold spring 1	239276	259481
Cold spring 2	239932	258983
Cold spring 3	240026	258938
Cold spring 4	239859	259158
Cold spring 6	239829	259231
Cold spring 7	239942	259106

2.2 Method

2.2.1 Geochemical Methodology

The water temperature, pH, and electrical conductivity (EC) were measured in situ. For this purposes, a portable digital thermometer, a pH meter and a digital conductivity meter were used.

The un-acidified water samples collected for geochemical analyses were filtered through 0.22-µm syringe filters to remove suspended particles and microbial contaminants. The aliquots of the filtered water were then collected into centrifugal vials for anion and cation analyses.

The concentrations of the major and trace cations, Ca^{2+}, K^{+}, Mg^{2+}, Fe^{2+}, Cr^{3+}, Al^{3+}, and Na+ present in the geothermal fluids were determined by using Agilent 4210 MP-AES (Microwave Plasma-Atomic Emission Spectroscopy) instrument.

The concentrations of the anions, F^{-}, Cl^{-}, Br^{-}, NO_3^{-}, SO_4^{2-} , and NO_2^{-} were determined by using a 930 Compact IC Flex (Ion Chromatography) instrument. The concentration of HCO_3^{-} was determined by a spectrophotometric method using Bromocresol green and hydrochloric acid[9] using a UV/VIS spectrophotometer.

The geothermal reservoir was characterized by processing the geochemical data using various geochemical diagrams and geothermometers.

2.2.2 Geophysical Methodology

Electrical Resistivity Survey

The mapping of the region was carried out using Schlumberger array configuration with two pairs of electrodes using Advanced Geosciences, Inc. (AGI) MINI STING Earth resistivity/ IP meter with 28 electrodes is used for 2D data acquisition. 2D linear profiles each of 270 m length, were obtained using the array setup with electrode spacing of 10 m.

Since the Geothermal field is located approximately in the NW-SE direction, the main profiling was done in the EW direction, while the cross profiling was done in the NS direction as the control.

Magnetic Survey

Magnetic measurements were performed using GEM Overhauser Magnetometer. The total number of magnetic stations were 120 with a spacing interval of 100 m.

The obtained results were then plotted and the IGRF values were calculated to find the corrected magnetic data.

Gravity Survey

The gravity surveys included 2040 gravity stations with electrode spacing of 10 m over a distance of 20 km.

The raw data were then corrected for several factors such as tide correction, tilt correction, drift correction, and terrain correction. Free-air anomaly, bouguer anomaly and complete bouguer anomaly graphs were plotted and analysed to find any information on the geological surface features.

Monte Carlo volumetric assessment

The Monte Carlo method was used to estimate the power generation in the near future using the best suitable values. The geothermal field surface area, thickness, temperature distribution, porosity, recovery factor, cut-off temperature, conversion efficiency factor of heat to electricity, and production time were considered for this estimation[1].

3 Results

3.1 Geochemistry of thermal and cold springs

The results of the In-situ measurements are summarized in Table 2.

Table 2: In-situ measurements

Location	pH	Surface temperature (°C)	EC (µS/cm)
Hot spring 1	5.54	33.3	1602
Hot spring 2	5.86	39.3	1506
Hot spring 3	6.15	37.6	1382
Hot spring 4	6.32	46.5	1670
Hot spring 5	6.71	39.2	1474
Hot spring 6	6.85	33.5	1446
Cold spring 1	6.25	27.4	1172
Cold spring 2	5.96	28.6	206
Cold spring 3	5.5	32.5	188
Cold spring 4	5.31	29.4	210
Cold spring 5	5.79	26.8	518
Cold spring 6	6.8	27.1	436

The major ion distributions in both types of waters of the thermal field are shown using the Schoeller diagrams in Figure 2.

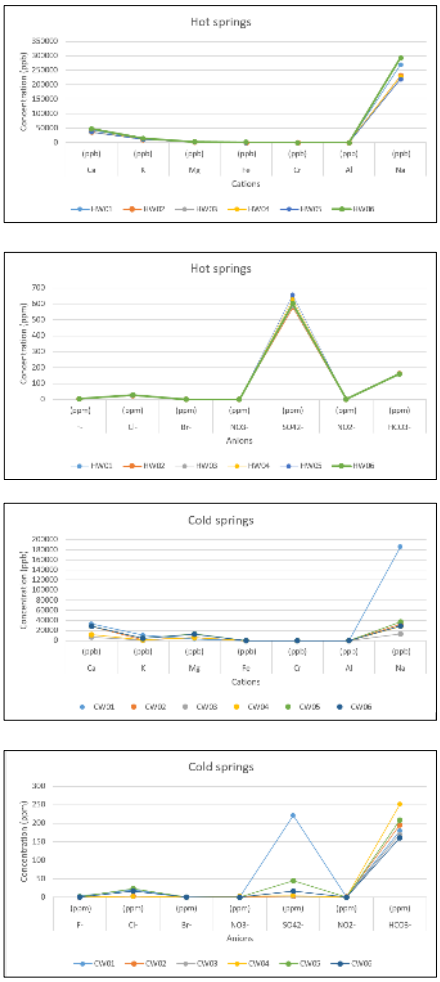

Figure 2: Schoeller Diagrams of the geothermal field

The samples from the field were then classified using a Piper plot as shown in figure 3.

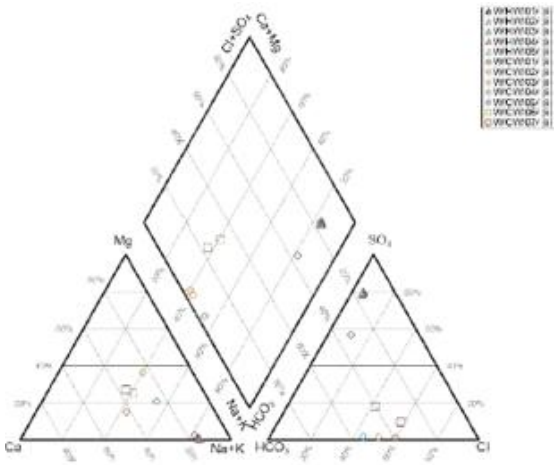

Figure 3: Classification of thermal water and cold water using a Piper diagram

The assessment of subsurface temperatures and water-rock equilibrium using Na-K-Mg Giggenbach 1988 ternary diagram is shown in figure 4.

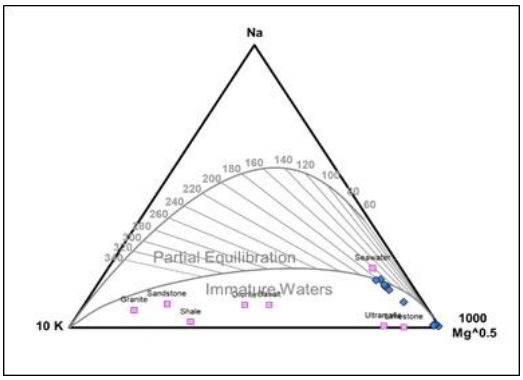

Figure 4: Na-K-Mg Giggenbach 1988 ternary diagram

3.2 Geophysics of geothermal field

3.2.1 Resistivity Results

The Wahawa Geothermal field consists of more than 10 surface manifestations. For the 2D data acquisition, 26 resistivity profiles were done in the area, of which 13 of them run through the geothermal field, from a previous study[3].

Those resistivity profiles were reprocessed, as shown in figure 5.

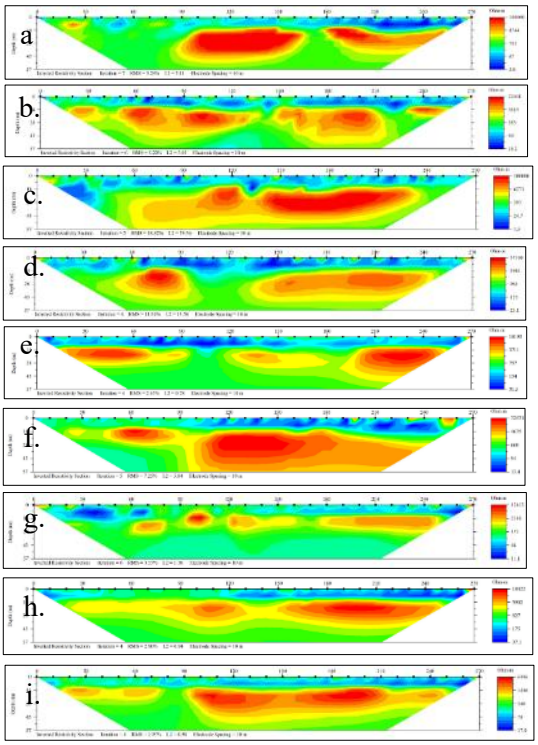

Figure 5: a. line10 b. line 11 c.line 12 d. line 13 e. line 14 f. line 15 g.line 16 h. line 17 i. line 18

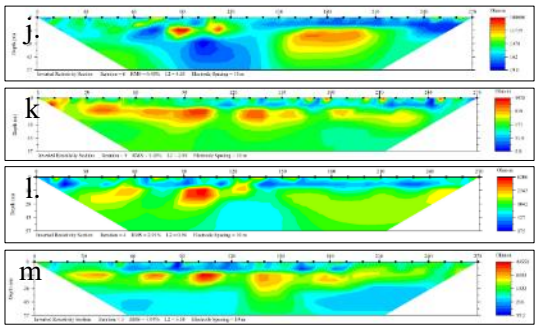

Figure 5: j. line 19 k. line 20 l. line 21 m. line 22

3.2.2 Magnetic Results

The figure 6 shows the magnetic intensity values mapped from the geothermal field.

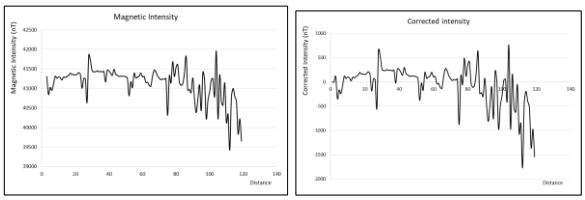

Figure 6: Plots of magnetic intensity and corrected intensity variation

3.2.3 Gravity results

The corrected gravity results are given in figure 7.

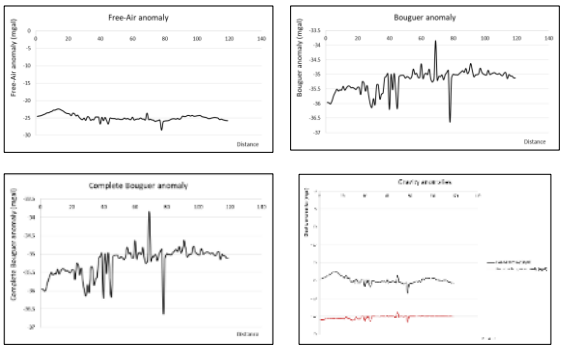

Figure 7: Results of the observed and calculated gravity anomalies

3.2.4 Monte Carlo volumetric assessment

The width of the geothermal belt was estimated to be 2-4 km across the boundary line and 2 km was taken as the reservoir thickness using a previous study in the field[10]. Subsurface temperatures determined by the geothermometers reached at 2-4 km of depth, also based on a thermal gradient of 35 °C/km. By considering the most likely value of the surface area to be 1 km^2 and the depth to be 2 km, the Monte Carlo simulation was operated. According to the subsurface temperatures obtained by the analysis, 200 °C was taken as the most likely reservoir temperature. As it is a low-temperature field, conversion efficiency was considered to be 5% for electrical power.

The Monte Carlo simulation was carried out and the results are shown in Table 3. The results point out that the volumetric assessment predicts with a 90% probability, that the reservoir could produce 2.6 MWe for 30 years.

Table 3: The summary of the potential of thermal energy from the field for 30 years

Most likely value	**2.6 MWe**
Highest Value	6.2 MWe
Lowest Value	1.6 MWe
Mean	3.8 MWe
Median	3.8 MWe
Standard deviation	0.9 MWe
Skewness	0.1 MWe^-2

The normalized probability distribution for a period of 30 years and the probability distribution for a cumulative power curve are shown in Figure 8.

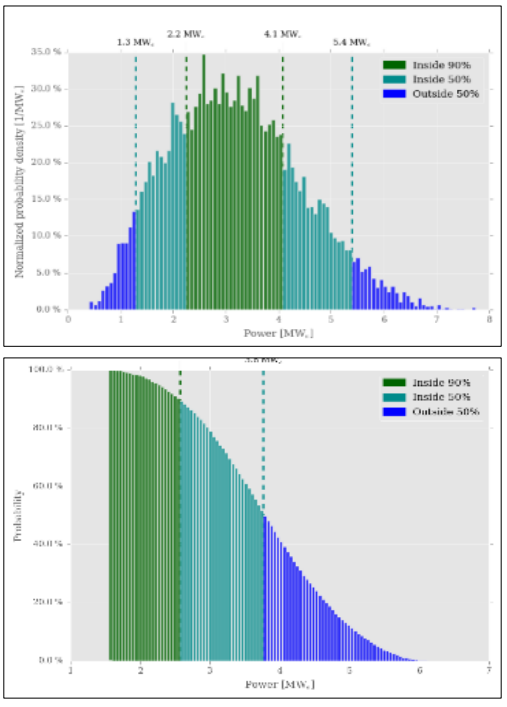

Figure 8: Normalized probability distribution of power and probability distribution of cumulative power for 30 years production, assuming a 1 km^2 reservoir area

4 Discussion

4.1 Geochemistry of the field

According to the table 2, the recorded wellhead temperatures of the geothermal springs range from 33 to 47 °C and the wellhead temperatures of the cold springs range from 27 to 33 °C. The recorded temperatures indicate that, this is a low-enthalpy geothermal system. A significant difference in the Electrical Conductivity (EC) can be observed between the thermal springs and the cold springs. The average values of EC of geothermal springs are relatively high and range between 1300 – 1700 µS/cm, while cold springs show values between 180 – 1400 µS/cm. Both water springs show slightly acidic conditions with pH ranging from 5 – 6.

From the Schoeller diagrams in figure 2, the results of the anions show a significantly higher concentration of SO_4^{2-} and a relatively high Cl^-, F^- was found in the thermal springs than cold water springs. A very low content of Br^- and undetectable amounts of NO_2^- were found in the thermal springs. The NO_3^- content was relatively higher in cold water samples. The cation analysis suggests, relatively higher concentrations of K and Ca and comparatively low concentrations of Mg for the thermal springs. Cr and Al are found in trace amounts. A considerable amount of Fe can be found in the water samples. Na is the dominant cation while SO_4^{2-} is the main anionic constituents in both hot and cold water samples.

The Piper plot from figure 3 indicates that, the thermal springs are rich in Na, K and SO_4^{2-} which, may be due to deep circulations and the cold water springs are rich in Na, K and HCO_3^- which, probably is due to the ion exchange between the thermal water and the deep underground water, as, also were shown in other geothermal field[11].

According to the calculations of the reservoir temperatures using geothermometry, Na/K Tonani 1980 gives maximum temperatures for cold springs and Na/K Giggenbach 1988 gives the maximum temperatures for hot springs in the field. The maximum temperature calculated for the thermal spring resevoir 186 °C, which potentially requires 697.2 kJ/mol of energy to heat, which therefore could be categorized as a low enthalpy geothermal energy.

4.2 Geophysics of geothermal field

4.2.1 Resistivity profiling

According to the resistivity profiles obtained from the survey area, as shown in figure 5, the information fracture zones in the field area could be obtained. The profile line-10 indicates the presence of highly resistive rocky zone with a sharp low resistive formation which divides the resistive basement near the centre of the profile, which could indicate a fracture zone. This may be due to the water bearing features extruded into the terrain underneath as a river flows over it.

The profiles line-10 and line-11 were taken across a river. The profile line-11 indicates the presence of a high resistive rock as well as several shallow surface fracture zones. The majority of the profile of line-12 is filled with a deep high resistive structure, which may be due to the underlying metamorphic rock.

The profile line-13 drawn in NS direction clearly shows the presence of a dominant wide fracture zone between highly resistive areas, which may be due to the geothermal manifestations. The profiling was made across a river as well. Similar features can also be spotted in line-14. A widespread low resistive fracture zones could be spotted in the profile of line-14, especially along the river site.

The profile line-15 indicates a presence of a high resistive deep basement area probably the metamorphic rock underneath, whereas the profile line-16 has some clusters of low resistive areas, between shallow high resistive regions, which could potentially suggest the presence of a reservoir. The profile line-17 gives indications of some wide near surface clusters of weak zones.

The fracture zones indicated by the profile line-18 in the EW direction and profile line-19 in NS directions coincides with each other, showing the presence of a deep fracture zone. The very low resistive region shown by the profile of line-19 could be a clear indication of the presence of a deep thermal reservoir. The profiles line-20, line-21 and line-22 clearly shows the presence of some near surface fractures, indicating the clustering of main fracture as well as the low resistive zone at the depth may indicate the presence of geothermal source.

The thermal waters from the relatively low resistive zones that extend to the surface from the deeper low resistive regions may have fluid

connections that enable extraction at shorter depths[10].

4.2.2 Magnetic results of the field

The figure 6 shows the magnetic intensity values mapped from the geothermal field. The magnetic intensity was relatively stable from 0 to 60 stations, with minor fluctuations, followed by increasing variability and several sharp drops between 60 and 130 stations.

The corrected profile flattens the average magnetic value near zero, making relative variations more apparent.

Minor, sharp positive anomalies likely show small, shallow magnetic bodies, such as surface dykes or intrusions.

Clear anomalies appear between 20 to 60 stations, and more significant negative anomalies dominate from 80 to 130 stations which indicates larger-scale geological structures, such as faulted blocks, intrusive rocks, or lithologic contacts.

4.2.3 Gravity values of the field

According to figure 7, the Free-Air anomaly values range from approximately –21 mGal to –30 mGal. This curve shows a generally decreasing trend from the beginning up to around 60 station of distance, followed by a noticeable sharp dip near 80 station and a minor increase again around 100 to 110 stations. These variations suggest the presence of dyke. The sharp anomaly near 80 station could indicate a subsurface low-density zone, such as a fault or a filled basin, but may also be partially influenced by terrain or tilt correction issues observed in earlier plots.

The Complete Bouguer anomaly is smoother, ranging from approximately –35 mGal to –39 mGal. This red curve removes the effects of elevation and terrain, offering a more accurate representation of subsurface density variations. Although the trend remains relatively stable, there are subtle changes throughout the profile. A slight gravity high is observed between 20 and 40 stations, which may suggest the presence of denser subsurface material, possibly an uplifted or compacted geological unit. The anomaly dips again around 80 station, consistent with the Free-Air anomaly, reinforcing the possibility of a real geological structure like a fault zone or a localized low-density body. From 100 to 120 stations, the Bouguer anomaly slowly rises, potentially indicating a more dense underlying formation or basement uplift such as the dyke.

4.3 Conceptual reservoir model

Based on the literature and the calculations from the surveys, a conceptual reservoir model can be developed for the Wahawa Geothermal field as given in figure 9. According to the evidence of manifestations, there is most likely a fault zone located along the dolerite dyke or across it. The spring waters due to precipitation from the highlands seep through the ground to deep high-temperature source built up as the thermal reservoir. The water collected at the reservoir is then presumably discharged to the surface from the thermal manifestations across the dyke area. The fracture zone facilitates the accumulation of water at the reservoir as it provides relatively high water flow rate with respect to the output flow rate at the surface thermal manifestations of hot water springs.

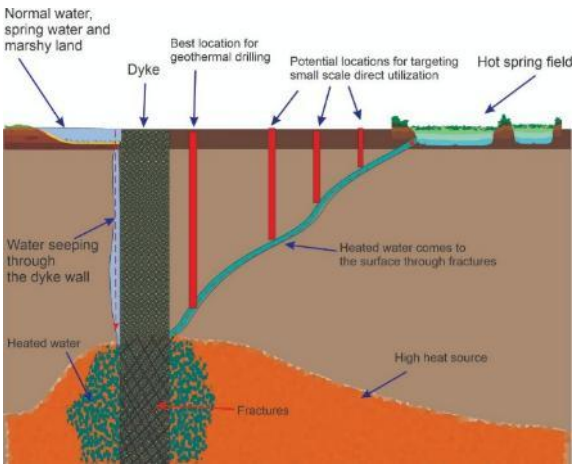

Figure 9: A conceptual model of the reservoir

5 Conclusions

The integrated geochemical assessment of the Wahawa geothermal field confirms that this is a low enthalpy geothermal system. The maximum temperature calculated for the thermal spring resevoir using geothermometry is 186 °C. The estimated energy required to potentially heat the reservoir is 697.2 kJ/mol. The Monte Carlo volumetric assessment predicts with a 90% probability that the reservoir could produce 2.6 MWe over a period of 30 years.

However, the exact area and the volume of the thermal reservoir and the depth of the fracture zone could not be exactly estimated from this study.

Further advanced geophysical studies combined with gravity, magnetotelluric method (MT),

vertical electrical sounding (VES), and, self-potential (SP) must be conducted to exactly delineate the geothermal area and to find the exact depth of the source and the reservoir.

Acknowledgement

This research was supported by the Rajarata University research grant 2024 (RJT/R&PC/2024/R/FOAS/05).

Prof. Meththika Vithanage, Faculty of Applied Sciences, University of Sri Jayewardenepura Sri Lanka for chemical analysis.

References

[1] P. S. Mangala and S. Wijetilake, “The Potential of Geothermal Energy Resources in Sri Lanka.”, Geothermal Training Programme, report 2011, no 34, 2011

[2] S. Patabendigedara, S. M. P. G. S. Kumara, and H. A. Dharmagunawardhane, “Geostructural Model for the Nelumwewa Thermal Spring; North Central Province, Sri Lanka a Geostructural Model for the Nelumwewa Thermal Spring: North Central Province, Sri Lanka,” *J. Geol. Soc. Sri Lanka*, vol. 16, pp. 19–27, 2014, [Online]. Available: https://www.researchgate.net/publication/273132920

[3] S. A. Samaranayake, N. Silva, U. Dahanayake, H. Wijewardane, and N. Subasinghe, “Delineation of Near Surface Water Flow Path of Wahawa Geothermal Field by Using 2D Inversion of Resistivity Data,” *J. Geosci. Environ. Prot.*, 2022, doi: 10.4236/gep.2022.108020.

[4] R. Chandrajith, J. A. C. Barth, N. D. Subasinghe, D. Merten, and C. B. Dissanayake, “Geochemical and isotope characterization of geothermal spring waters in Sri Lanka: Evidence for steeper than expected geothermal gradients,” *J Hydrol.*, vol. 476, pp. 360–369, Jan. 2013,doi:10.1016/j.jhydrol.2012.11.004.

[5] Sri Lanka Sustainable Energy Authority, “Sri Lanka Sustainable Energy Authority,” Web : www.energy.gov.lk +94. Accessed: Apr. 15, 2025. [Online]. Available: www.energy.gov.lk

[6] A. Senaratne and D. Chandima, “Exploration of a Potential Geothermal Resource at Wahawa Padiyatalwa Area Sri Lanka.”, 2011

[7] M. Abeysinghe, M. Thilakarathna, A. M. A. M. Abeysinghe, M. P. Thilakarathna, C. B. Dissanayake, and N. D. Subasinghe, “Application of Geological, Geochemical, and Geophysical Techniques in Geothermal Explorations of Sri Lanka-A review,” *J. Geol. Soc. Sri Lanka*, vol. 23, no. 2, pp. 11–22, 2023, doi: 10.4038/jgssl.v231.64.

[8] C.B. Dissanayake, and H.A.H. Jayasena, "Origin of geothermal systems of Sri Lanka," Geothermics, vol. 17, no. 4, 1988, doi: 10.1016/0375-6505(88)90050-8.

[9] H. Yang, T. Mishima, S. Katazakai, and M. Kagabu, “Analytical approach using a chemical equilibrium formula and geochemical modeling for alkalinity measurements of small natural water samples,” *Appl. Geochemistry*, vol. 148, 2023, doi: 10.1016/j.apgeochem.2022.105535.

[10] B. A. Hobbs *et al.*, “Geothermal Energy Potential in Sri Lanka: a Preliminary Magnetotelluric Survey of Thermal Springs,” *J. Geol. Soc. Sri Lanka*, vol. 15, no. April 2015, pp. 69–83, 2013.

[11] D. T. Jayawardana, D. T. Udagedara, A. A. M. P. Silva, H. M. T. G. A. Pitawala, W. K. P. Jayathilaka, and A. M. N. M. Adikaram, “Mixing geochemistry of cold water around non-volcanic thermal springs in high-grade metamorphic terrain, Sri Lanka,” *Chemie der Erde*, vol. 76, no. 4, pp. 555–565, Dec. 2016, doi: 10.1016/j.chemer.2016.10.003.